

## Studies on Some Low-Lying Levels of $\text{Ne}^{21}\dagger$

A. J. HOWARD,\* J. P. ALLEN,‡ AND D. A. BROMLEY

*Nuclear Structure Laboratory, Yale University, New Haven, Connecticut*

AND

J. W. OLNES AND E. K. WARBURTON

*Brookhaven National Laboratory, Upton, New York*

(Received 18 January 1967)

The  $\text{Ne}^{21}$  states below an excitation energy of 5 MeV have been studied via the  $\text{Ne}^{20}(d,p)\text{Ne}^{21}$  and  $\text{Ne}^{20}(d,p\gamma)\text{Ne}^{21}$  reactions with deuteron bombardment energies below 4 MeV. Angular-distribution measurements performed on the unresolved proton groups corresponding to formation of the 2.790- and 2.797-MeV  $\text{Ne}^{21}$  states display  $l_n=0$  stripping characteristics. Based on the observed relative intensities of population for these two states in previous studies, this measurement is interpreted as direct evidence for a  $J^\pi=\frac{1}{2}^+$  assignment to the 2.797-MeV  $\text{Ne}^{21}$  state. Two-parameter proton-gamma time-coincidence measurements have been carried out to investigate the de-excitation branching ratios for the 1.75-, 2.87-, 3.67-, 3.74-, 3.89-, 4.53-, and 4.73-MeV  $\text{Ne}^{21}$  states. Proton-gamma angular-correlation studies were performed in a colinear geometry at  $E_d=3.0$  MeV. The results confirm previous  $J=\frac{3}{2}$  determinations for the 1.75-MeV  $\text{Ne}^{21}$  state and indicate a value  $x=+(0.11\pm 0.03)$  for the multipole amplitude ratio of the  $1.75\rightarrow 0.350$  transition. They also indicate  $J=\frac{3}{2}$  or  $\frac{5}{2}$  for both the 3.67- and 3.74-MeV states and  $J\geq\frac{3}{2}$  for the 3.89-MeV state. All radiations originating from the 2.790-MeV state appeared isotropic within experimental uncertainties, and the present results indicate only that  $J\leq\frac{5}{2}$  for this state. The results of these and previous studies are compared with existing collective-model predictions concerning the  $\text{Ne}^{21}$  nuclear system.

### I. INTRODUCTION

PROPERTIES of the  $\text{Ne}^{21}$  levels below an excitation energy of 5 MeV have been studied recently on several occasions.<sup>1-10</sup> Some of the more recent of these investigations<sup>3,7-9</sup> have conclusively established the existence of two close-lying states with excitation energies in  $\text{Ne}^{21}$  of 2.790 and 2.797 MeV. This discovery has resolved ambiguities concerning previous spectroscopic information which assumed the existence of only one level in this energy region.<sup>1,2</sup> It has been assumed<sup>3,6-9</sup> on the basis of the lifetime and branching-ratio information<sup>6-9</sup> available on each of these two states that the observed<sup>10,11</sup>  $l_n=0$  stripping characteristics associated with the angular distribution of the two (unresolved)

proton groups in the  $\text{Ne}^{20}(d,p)\text{Ne}^{21}$  reaction belong with the 2.797-MeV state and hence that  $J^\pi=\frac{1}{2}^+$  for this level. Although this assumption is most probably correct, it has not been directly confirmed because ( $d,p$ ) angular distributions were measured at higher deuteron energies than those used to investigate the relative feeding of the 2.790- and 2.797-MeV levels. Recent angular-correlation studies<sup>9</sup> on the  $\text{O}^{18}(\alpha,n\gamma)\text{Ne}^{21}$  reaction have been interpreted to give  $J=\frac{3}{2}$  for the  $\text{Ne}^{21}$  2.790-MeV level, and the analysis of these correlations was dependent on an assumption of  $J=\frac{1}{2}$  for the 2.797-MeV level. This gave additional impetus to further investigation of the spin of the 2.797-MeV level.

The presently available information concerning the bound  $\text{Ne}^{21}$  states with  $E_x>2.8$  MeV is, in general, very ambiguous. The present situation regarding the static properties of known  $\text{Ne}^{21}$  states below 5-MeV excitation energy is summarized in Table I. Data are taken from Refs. 1-14.

The investigation to be reported herein was composed of three distinct studies. The first study, reported in Sec. II, was carried out to investigate further the spin associated with the 2.797-MeV level in  $\text{Ne}^{21}$ : The angular distributions of the (unresolved) proton groups in the  $\text{Ne}^{20}(d,p)\text{Ne}^{21}$  reaction corresponding to formation of the 2.790- and 2.797-MeV states were measured with incident deuteron energies of 1.63, 2.19, 2.70, and 3.20 MeV at the reaction volume, these values of beam

† Work supported in part by the U. S. Atomic Energy Commission.

\* On leave of absence (1966-1967) from Trinity College, Hartford, Connecticut.

‡ Present address: Physics Department, University of Washington, Seattle, Washington.

<sup>1</sup> D. Pelte, B. Povh, and W. Scholz, Nucl. Phys. **55**, 322 (1964).

<sup>2</sup> A. J. Howard, D. A. Bromley, and E. K. Warburton, Phys. Rev. **137**, B32 (1965).

<sup>3</sup> D. Pelte, B. Povh, and B. Schurlein, Nucl. Phys. **73**, 481 (1965).

<sup>4</sup> D. Pelte and B. Povh, Nucl. Phys. **73**, 492 (1965) and D. Pelte (private communication).

<sup>5</sup> R. L. Robinson, P. H. Stelson, F. K. McGowan, J. L. C. Ford, Jr., and W. T. Milner, Nucl. Phys. **74**, 281 (1965).

<sup>6</sup> J. G. Pronko, W. C. Olsen, and J. T. Sample, Nucl. Phys. **83**, 321 (1966).

<sup>7</sup> P. J. M. Smulders and T. K. Alexander, Phys. Letters **21**, 664 (1966).

<sup>8</sup> R. Kömpf, Phys. Letters **21**, 671 (1966).

<sup>9</sup> J. G. Pronko, C. Rolfs, and J. J. Maier, Nucl. Phys. **A94**, 561 (1967).

<sup>10</sup> D. J. Pullen, A. Sperduto, and E. Kashy, Bull. Am. Phys. Soc. **10**, 38 (1965); D. J. Pullen (private communication).

<sup>11</sup> H. B. Burrows, T. S. Green, S. Hinds, and R. Middleton, Proc. Phys. Soc. (London) **A69**, 310 (1956).

<sup>12</sup> W. M. Deuchars and D. Dandy, Proc. Phys. Soc. (London) **77**, 1197 (1961).

<sup>13</sup> J. M. Freeman, Phys. Rev. **120**, 1436 (1960).

<sup>14</sup> R. D. Bent, J. E. Evans, G. C. Morrison, and I. J. Van Heerden, in *Proceedings of the Third Conference on Reactions Between Complex Nuclei*, edited by A. Ghiorso, R. M. Diamond, and H. E. Conzett (University of California Press, Berkeley, California, 1963), p. 417.

energy being in a range where it is known from  $\text{Ne}^{20}(d,p\gamma)\text{Ne}^{21}$  studies<sup>2</sup> that the 2.797-MeV state is populated much more intensely than is the 2.790-MeV state. The second study, reported in Sec. III A, provided the data for improved branching-ratio determinations concerning several of the  $\text{Ne}^{21}$  states below 5-MeV excitation energy; two-parameter proton-gamma ( $p\text{-}\gamma$ ) time-coincidence measurements were performed on the  $\text{Ne}^{20}(d,p\gamma)\text{Ne}^{21}$  reaction at bombardment energies 2.2 and 3.4 MeV in a favorable geometry ( $\theta_p=90^\circ, \theta_\gamma=45^\circ$ ). The third study, reported in Sec. III B, involved  $p\text{-}\gamma$  angular-correlation measurements on the  $\text{Ne}^{20}(d,p\gamma)\text{Ne}^{21}$  reaction, which were carried out in a colinear geometry ( $\theta_p \simeq 180^\circ$ ) at  $E_d=3.0$  MeV. The experimental information relating to the bound states of  $\text{Ne}^{21}$  is discussed in Sec. IV from a strong-coupling collective-model viewpoint.

## II. $\text{Ne}^{20}(d,p)\text{Ne}^{21}$ PROTON ANGULAR-DISTRIBUTION MEASUREMENTS

### A. Orientation

The angular distributions of protons in the  $\text{Ne}^{20}(d,p)\text{Ne}^{21}$  reaction have been measured by Burrows *et al.*<sup>11</sup> at  $E_d=8.5$  MeV and by Pullen *et al.*<sup>10</sup> at  $E_d=7.1$  MeV. Analyzing the observed distribution of a proton group corresponding to formation of a  $\text{Ne}^{21}$  level at  $E_x=2.78 \pm 0.05$  MeV via application of the plane-wave Born approximation (PWBA), Burrows *et al.*<sup>11</sup> reported unambiguous  $l_n=0$  stripping characteristics and consequently assigned  $J^\pi=\frac{1}{2}^+$  to this level. Pullen *et al.*<sup>10</sup> found similar behavior upon distorted-wave Born-approximation (DWBA) analyses of their distribution measurements corresponding to a  $\text{Ne}^{21}$  level at  $2.800 \pm 0.007$  MeV.

It is therefore well established that a  $\frac{1}{2}^+$  state does exist near 2.800 MeV in  $\text{Ne}^{21}$ ; the only difficulty is the proper identification of this assignment with one (or both) of the 2.790- and 2.797-MeV states. It is known that in the  $\text{Ne}^{20}(d,p)\text{Ne}^{21}$  reaction the 2.797-MeV state is populated considerably stronger than the 2.790-MeV level for incident deuteron energies less than  $\sim 3$  MeV. For instance, when reanalyzed with recent branching-ratio information,<sup>7-9</sup> data from a previous study<sup>2</sup> on the  $\text{Ne}^{20}(d,p\gamma)\text{Ne}^{21}$  reaction indicate that the 2.797-MeV level is populated about nine times as intensely as the 2.790-MeV level throughout the range of incident deuteron energies  $0.9 \leq E_d \leq 2.9$  MeV. This conclusion is consistent with other results at  $E_d=2.05$  MeV<sup>8</sup> and 2.24 MeV.<sup>3</sup> The suggested<sup>3,7-9</sup> identification of the 2.797-MeV state as the  $\frac{1}{2}^+$  state is based on the fact that relative ( $d,p$ ) cross sections for populating different final states are usually observed to be insensitive to deuteron energy, so that it appears quite likely that the 2.797-MeV level is the one observed at  $E_d=7.1$  and 8.5 MeV. However, we feel that it is desirable to make a more direct association of the  $l_n=0$  stripping

TABLE I. Summary of previous information on the static properties of  $\text{Ne}^{21}$  states below 5-MeV excitation energy.

$E_x$ (MeV)	Reference	$J^\pi$	Reference
0	...	$\frac{3}{2}^+$	12
$0.3502 \pm 0.0008$	5	$\frac{1}{2}^+$	2,10,11
$1.750 \pm 0.007$	13	$\frac{1}{2}^+$	1,2,6,14
$2.790 \pm 0.002$	7,8	$(\frac{1}{2})$	4
		$\frac{3}{2}^+$	9
$2.797 \pm 0.002$	7,8	$(\frac{1}{2}^+)$	10,11
$2.870 \pm 0.007$	13	$\frac{3}{2}^+$	6,9
$3.666 \pm 0.007$	13	$\frac{1}{2}^+$	2
		$\frac{3}{2}^+$	4
$3.737 \pm 0.007$	13	$(\frac{1}{2}^+)$	2
		$\frac{3}{2}^+$	4
$3.889 \pm 0.007$	13	$\frac{3}{2}^+$	3
$4.435 \pm 0.007$	13	$\frac{3}{2}^+$	3,9
$4.528 \pm 0.007$	13	$(\frac{1}{2}^+)$	4
		$\frac{3}{2}^+$	10
$4.685 \pm 0.009$	13	$\frac{1}{2}^+$	10
$4.729 \pm 0.008$	13	$\frac{1}{2}^+$	2,10

pattern with the 2.797-MeV level by repeating the angular-distribution measurements at deuteron energies in the range  $0.9 \leq E_d \leq 2.9$  MeV.

### B. Procedures

Beams from the Brookhaven National Laboratory 3-MeV Van de Graaff accelerator were employed for all the present studies.  $\text{Ne}^{20}$  gas targets of  $>99\%$  isotopic and elemental constitution were used for all studies concerning  $\text{Ne}^{21}$ ; in the particle distribution measurements reported in this section, a  $\text{Ne}^{22}$  gas target of purities similar to those quoted above was also employed.

Retained by a 0.1-mil-thick beam entrance window, the target gases were contained within the chamber illustrated in Fig. 1 at 10 cm of mercury absolute pressure. Two solid-state charged-particle detectors were mounted independently in this chamber and operated directly within the target gas. The first counter, which was used to measure the proton angular distributions, was attached to an externally controlled angular-distribution table, whose position was continuously variable from  $\theta_p=0^\circ$  to  $135^\circ$  with respect to the beam vector. The angular position of this detector was determined to within  $1^\circ$  by means of an external scale and pointer system. The second, monitor counter was fixed at  $90^\circ$  and was used for a control-normalization source.

Collimation of the beam and definition of the scattering volume viewed by the detectors ("reaction volume") were achieved by pairs of circular 1.5-mm-diam tantalum apertures, which were located immediately after the beam entrance window and determined the beam profile; two more were placed before each detector to define the extent of the (angle-dependent) reaction volume and hence to limit the angular divergence of emergent protons to  $\sim 1^\circ$ . Each of the two collimator-detector assemblies was enclosed in a tantalum jacket so that protons (and deuterons) incident upon the

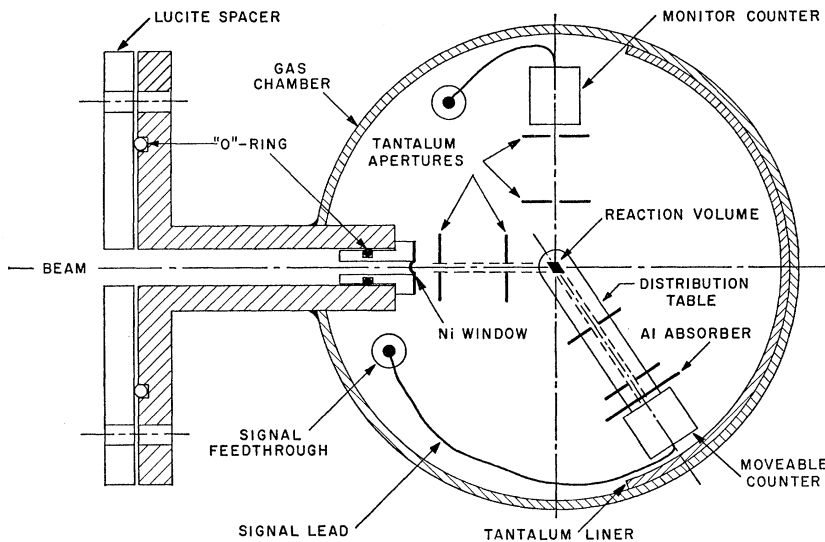


FIG. 1. Schematic diagram of the gas scattering chamber employed for the proton angular-distribution measurements.

detector necessarily had passed through the two apertures.  $\alpha$ -particle groups originating in the  $(d,\alpha)$  reaction were removed from the view of each particle detector by insertion of a 1-mil-thick aluminum absorber foil between the second aperture and the detector.

The entire target assembly was electrically isolated by means of a Lucite spacer placed between it and the beam tube, which permitted integration of the total incident-beam current. This method of current integration was selected because the purpose of the experiment was the determination of relative intensities for a given proton group at extreme forward angles. Normalization factors for datum points taken at various angles as deduced from this current integration were found in general to be in excellent agreement with those obtained from the spectra collected by the monitor detector.

Upon appropriate amplification and shaping, pulses originating from each of these detectors were stored in separate RIDL 400-channel analyzers. The relative intensity of each group of interest in a given spectrum was obtained by determining the number of counts in the observed peak, correcting this number for analyzer dead time, multiplying the result by  $\sin\theta_p$  (which corrects to first order for the angular-dependent number of target nuclei viewed by the detector), and finally normalizing these results according to the total integrated beam charge recorded during the measurement.

A typical distribution measurement involved obtaining data in  $5^\circ$  and  $10^\circ$  steps from  $\theta_p=8^\circ$  to  $123^\circ$  in the laboratory system. Positive identifications of all proton groups to be discussed below were made by comparison of the experimentally measured and kinematically expected energies at the various angles studied.

In order to extend the distributions as obtained above to an extreme backward angle ( $\theta_p \approx 165^\circ$ ), relevant proton spectra obtained with the  $\theta_p=180^\circ$  chamber described in Sec. III B of this paper were compared,

after appropriate normalizations, with similar spectra obtained with the  $\theta_p=90^\circ$  chamber discussed in Sec. III A. The magnitudes of the uncertainties in the (mostly geometrical) normalization factors entering this computation of relative intensities at  $\theta_p=90^\circ$  and  $165^\circ$  were generously estimated, and so the resulting  $\theta_p=165^\circ$  data points have the relatively large uncertainties depicted in Fig. 2.

### C. Results

The first measurements performed in the above fashion were on the proton groups corresponding to formation of the 1.02- and 0-MeV  $\text{Ne}^{23}$  states in the  $\text{Ne}^{22}(d,p)\text{Ne}^{23}$  reaction. The previous studies by Burrows *et al.*<sup>11</sup> and by Pullen *et al.*<sup>10</sup> have each indicated unambiguous  $l_n=0$  and 2 stripping characteristics, respectively, in the formation of these energetically isolated states, and so the present study of these distributions was carried out for comparative purposes. Measurements were performed with incident deuteron energies of 2.19, 2.70, and 3.20 MeV at the reaction volume. Results of the latter measurement are presented in the upper half of Fig. 2. Using values of the interaction radius parameter  $R$  comparable to those used by Burrows *et al.*<sup>10</sup> ( $R=6.5 \times 10^{-13}$  cm and  $6.1 \times 10^{-13}$  cm for the interactions populating the respective 1.02- and 0-MeV  $\text{Ne}^{23}$  levels), good PWBA fits are obtained for these 1.02- and 0-MeV  $\text{Ne}^{23}$  proton distributions with  $l_n=0$  and 2, respectively (see Fig. 2). Similarly good fits were obtained for the distributions measured at the lower bombardment energies.

Angular-distribution measurements on the  $\text{Ne}^{20}(d,p)\text{Ne}^{21}$  reaction were then performed at incident deuteron energies of 1.63, 2.19, 2.70, and 3.20 MeV on the (unresolved) 2.790- and 2.797-MeV and on the 0.350-MeV  $\text{Ne}^{21}$  proton groups, the latter of which is known from previous studies at higher bombardment energies<sup>9,10</sup>

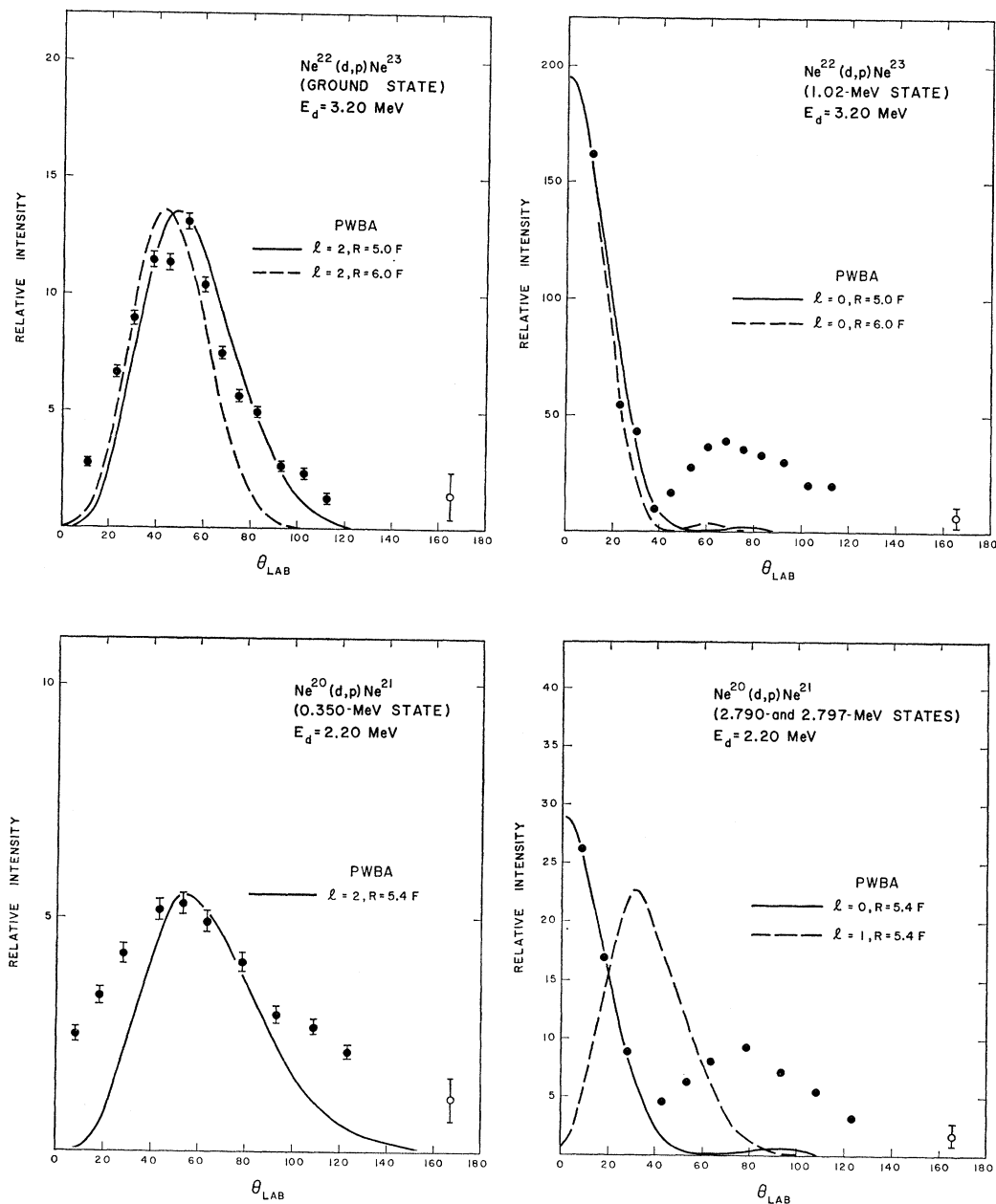


FIG. 2. Proton angular distributions observed in the  $\text{Ne}^{22}(d,p)\text{Ne}^{23}$  reaction at  $E_d = 3.20$  MeV (upper portion) and in the  $\text{Ne}^{20}(d,p)\text{Ne}^{21}$  reaction at  $E_d = 2.20$  MeV (lower portion). The solid points were obtained using the scattering chamber illustrated in Fig. 1, and the open points were subsequently obtained by comparison of proton spectra viewed in  $\theta_p = 90^\circ$  and  $\theta_p = 165^\circ$  chambers as discussed in the text. Arguments presented in the text indicate that the "combined" distribution illustrated in the lower-right portion of the figure is to be associated with formation of the 2.797-MeV state. Plane-wave Born-approximation fits to the data are illustrated for the indicated values of the interaction radius parameter  $R$  and the angular-momentum transfer  $l$ .

to display  $l_n = 2$  stripping characteristics in its formation via this reaction. Representative distributions (taken at 2.19 MeV) are presented in the bottom half of Fig. 2. Analyses identical to those applied to the  $\text{Ne}^{22}(d,p)\text{Ne}^{23}$  data discussed above strongly indicate  $l_n = 0$  and 2 stripping characteristics in the formation of the 2.790-, 2.797-MeV composite and the 0.350-MeV state,

respectively. This is equally true of the distribution analyses for data obtained at the other three bombardment energies. In view of the relative population arguments presented in Sec. II A of this paper and well documented elsewhere,<sup>2</sup> we conclude that the assignment  $J^\pi = \frac{1}{2}^+$  to the 2.797-MeV  $\text{Ne}^{21}$  state has been unequivocally confirmed.

### III. STUDIES ON THE $\text{Ne}^{20}(d,p\gamma)\text{Ne}^{21}$ REACTION

#### A. Gamma-Ray Branching-Ratio Measurements

The deuteron beams were incident upon a 0.1-mil-thick nickel entrance window attached to a previously described gas cell,<sup>2</sup> which was modified so as to view protons at  $\theta_p=90^\circ$ .  $\text{Ne}^{20}$  gas was maintained at 10 cm of mercury absolute pressure in this cell, and charged particles emanating from the reaction volume were observed by a 0.25-cm<sup>2</sup> solid-state detector immersed in the target gas itself. This counter was located at  $\theta_p=90^\circ$  and at a distance of 5 cm from the center of the reaction volume. A conical tantalum collimator shielded the detector from directly viewing either the nickel entrance window or the tantalum beam stop at the rear of the chamber; the proton angular divergence associated with this system was  $\pm 10^\circ$ . A 0.5-mil-thick aluminum foil was placed before the face of the detector so as to absorb the  $\alpha$ -particle groups from the  $\text{Ne}^{20}(d,\alpha)\text{F}^{18}$  reaction, for which  $Q_m=+2.784$  MeV. This foil allowed passage in the present measurements of the proton groups corresponding to formation of

$\text{Ne}^{21}$  states below 5-MeV excitation energy via the  $\text{Ne}^{20}(d,p)\text{Ne}^{21}$  reaction, for which  $Q_m=+4.534$  MeV.

Gamma radiations were examined by means of a 5 $\times$ 5-in. NaI(Tl) spectrometer located outside the target chamber at  $\theta_\gamma=45^\circ$  to the deuteron-beam vector. The front face of this detector was situated 5 cm from the "effective" reaction volume, which represented the reaction volume directly viewed by the particle detector.

A two-parameter proton-gamma coincidence measurement was performed at  $E_d=3.40$  MeV, and a similar study was also carried out at  $E_d=2.10$  MeV. A TMC 16 384-channel pulse-height analyzer was used in conjunction with external fast-slow coincidence circuitry operating with  $\sim 60$ -nsec resolving time; a 256-channel ( $\gamma$ -ray) by 64-channel (proton) data array was employed for these measurements. Each experiment was carried out with a 2-nA deuteron beam current: The real-to-random coincidence ratios associated with proton-gamma coincidences were typically  $\sim 20:1$ , and elapsed time for each measurement was 20 h. The data were recorded on magnetic tapes, and the 256 $\times$ 64-

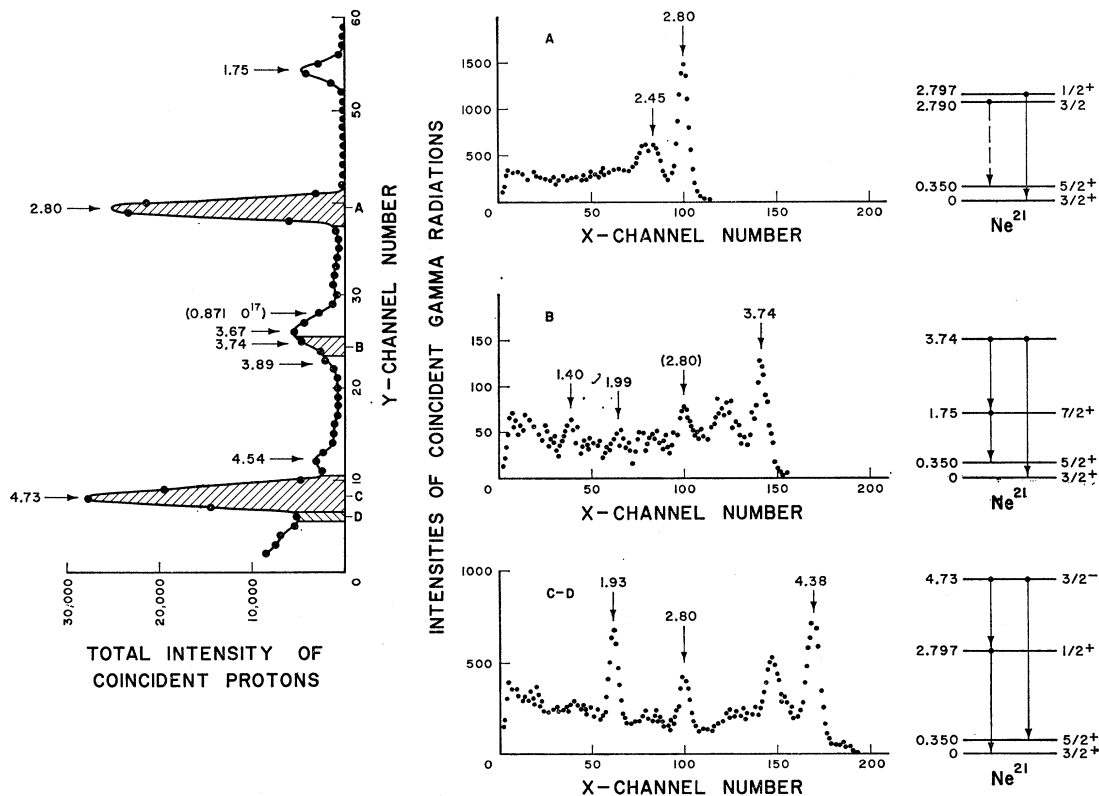


FIG. 3.  $\gamma$ -ray spectra observed in time coincidence with selected regions of the proton spectrum in the  $\text{Ne}^{20}(d,p\gamma)\text{Ne}^{21}$  reaction at  $E_d=3.40$  MeV,  $\theta_\gamma=45^\circ$ , and  $\theta_p=90^\circ$ . The proton groups observed to be in coincidence with  $\gamma$  radiation in the energy range 0.5 to 5 MeV are displayed in the left section of the figure; here the numeric labels identify the proton groups according to their excitation energy (MeV) in  $\text{Ne}^{21}$ , and the alphabetic labels refer to specific (shaded) foreground or background regions of the proton spectrum. The  $\gamma$  rays observed to be coincident with selected regions of the proton spectrum are displayed in the center section of the figure; here alphabetic labels correspond to those indicated in the coincident proton spectrum, and the numeric labels identify observed  $\gamma$ -ray transition energies (MeV). These transitions corresponding to the real coincidences are positioned in the  $\text{Ne}^{21}$  level schemes presented in the right section of the figure.

channel data arrays were subsequently analyzed with the use of an IBM 7094 computer. This data analysis procedure, which essentially consists of determining the 256-channel  $\gamma$ -ray spectra that were observed in time coincidence with the relevant proton groups, has been discussed in detail elsewhere.<sup>15</sup> Results of the  $E_d=3.40$ -MeV measurement are exemplified in Fig. 3.

Extraction of branching ratios from the resultant  $\gamma$ -ray spectra was done with the aid of established  $\gamma$ -ray (photofraction) efficiency curves.<sup>16</sup> Detailed considerations of sum-peak contributions, which were pronounced in some cases because of the geometry employed, were made in the extraction procedure. Finally, it was estimated that angular-correlation corrections applicable to the observed branching ratios were negligible.

The  $\gamma$ -ray branching ratios presented in Table II for the 3.74-, 3.89-, 4.53-, and 4.73-MeV Ne<sup>21</sup> states were derived from the above data. Branching-ratio data given in Table II for the 1.75-, 2.87-, and 3.67-MeV levels were those obtained from the measurement described in the next subsection, which gave superior counting statistics as regards these latter three states. Also given in Table II are the branching ratios obtained from previous investigations as well as the averages of these previous and the present data.

### B. Proton-Gamma Angular-Correlation Measurements

Ne<sup>20</sup> gas was maintained at 33 cm of mercury absolute pressure in a 0.625-cm-diam by 2-cm-long cylindrical gas cell located with its axis of revolution colinear with the beam vector. The cylindrical shell wall was 0.1-cm-thick brass, and the chamber ends were defined by 0.04-mil-thick 0.625-cm-diam nickel entrance and exit windows. This cell was centrally situated in the angular-correlation chamber described by Olness and Warburton.<sup>15</sup> For this study, carried out in method II geometry of Litherland and Ferguson,<sup>17</sup> the charged particles were detected at  $\theta_p=(165\pm 6)^\circ$  by an annular detector of 1.0-cm<sup>2</sup> active area, which was located external to the gas cell itself. Deuterons scattered by the entrance and exit foils as well as those scattered by the target gas were removed from the view of the detector by an appropriately placed (annular) 1.5-mil-thick aluminum absorber foil; all  $\alpha$ -particle groups associated with the Ne<sup>20</sup>( $d,\alpha$ )F<sup>18</sup> reaction were also stopped by this absorber.

The relative intensities of proton groups corresponding to formation of the Ne<sup>21</sup> states below 4-MeV excitation energy were measured as a function of deuteron-

TABLE II. Summary of observed  $\gamma$ -ray branching ratios in Ne<sup>21</sup>.

Initial state (MeV)	Final state (MeV)	Present work	Previous work; reference	Average
4.73	0	<4		<4
	0.350	84±1	80±2; 3	83±1
	1.75	<1		<1
	2.790	<2		<2
	2.797	16±1	20±2; 3	17±1
	2.87	<1		<1
4.69		Not observed <sup>a</sup>	Not observed <sup>a</sup>	...
4.53	0	22±4		22±4
	0.350	78±4	(100); 3	78±4
	1.75	<4		<4
	2.790	<3		<3
	2.797	<4		<4
	2.87	<2		<2
4.44	0	Not observed <sup>b</sup>		
	0.350			
	1.75		~30; 3 <sup>b</sup>	~30
	2.790			
	2.797			
	2.87		~70; 3 <sup>b</sup>	~70
3.89	0	23±5	26±5; 3	24±4
	0.350	77±5	74±5; 3	76±4
	1.75	<10		<10
	2.790	<6		<6
	2.797	<6		<6
	2.87	<3		<3
3.74	0	94±1	50±15; 3	92±2
	0.350	<9	15±15; 3	<9
	1.75	6±1	35±15; 3	8±2
	2.790	<3		<3
	2.797	<4		<4
	2.87	<2		<2
3.67	0	<7	≤12; 3	<7
	0.350	64±3	56±5; 3	61±3
	1.75	<3		<3
	2.790	36±3	44±5; 3	39±3
	2.797	<5		<5
	2.87	<3		<3
2.87	0	<10		<10
	0.350	30±6	33±3; 3,9	32±3
	1.75	70±6	67±3; 3,9	68±3
2.797	0	(100) <sup>o</sup>	100; 7-9	100
	0.350		<5; 7-9	<5
	1.75	<1		<1
2.790	0	(15) <sup>e</sup>	15±4; 7-9	15±4
	0.350	(85) <sup>e</sup>	85±4; 7-9	85±4
	1.75	<1		<1
1.75	0	6.8±0.7	6±1; 1	6.5±0.6
	0.350	93.2±0.7	94±1; 1	93.5±0.6

<sup>a</sup> The data summarized in Table I of Ref. 2 indicate that the 4.73- and 4.69-MeV Ne<sup>21</sup> states are populated in the approximate ratio 15:1 at  $\theta_p=90^\circ$ ,  $E_d=7.1$  MeV in the Ne<sup>20</sup>( $d,p$ )Ne<sup>21</sup> reaction. Assuming this ratio is essentially the same at the presently considered bombardment energies, the 4.73 → 0.350 transition occludes the possible 4.69 → 0.350 transition in the present measurements.

<sup>b</sup> Ambiguities associated with the data of Ref. 3 concerning the 4.53- and 4.44-MeV states are resolved in the present experiment by establishing the branching ratio of the 4.53-MeV level. Consequently, the data displayed in Fig. 6 of Ref. 3 have been used to estimate the branching ratio of the 4.44-MeV state as presented herein.

<sup>c</sup> These quoted branching ratios are assumed, on the basis of the results of Refs. 7-9, for the purpose of computing the indicated limits.

bombardment energy in the interval  $E_d=2.5$  to 3.5 MeV. Results for the 1.75-MeV, the unresolved 2.790- and 2.797-MeV, and the unresolved 3.67- and 3.74-MeV Ne<sup>21</sup> proton groups are illustrated in Fig. 4. Intensities for each of the 2.790-, 2.797-MeV and 3.67-, 3.74-MeV proton groups reach a relative maximum near  $E_d=3.00$  MeV, and consequently an angular-correlation measurement was carried out at this bombardment energy.

<sup>15</sup> J. W. Olness and E. K. Warburton, Phys. Rev. **151**, 792 (1966).

<sup>16</sup> S. H. Vegors, L. L. Marsden, and R. L. Heath, Phillips Petroleum Company Report No. IDO-16370, 1958 (unpublished); F. C. Young, H. T. Heaton, G. W. Phillips, P. D. Forsyth, and J. B. Marion, Nucl. Instr. Methods **44**, 109 (1966).

<sup>17</sup> A. E. Litherland and A. J. Ferguson, Can. J. Phys. **39**, 778 (1961).

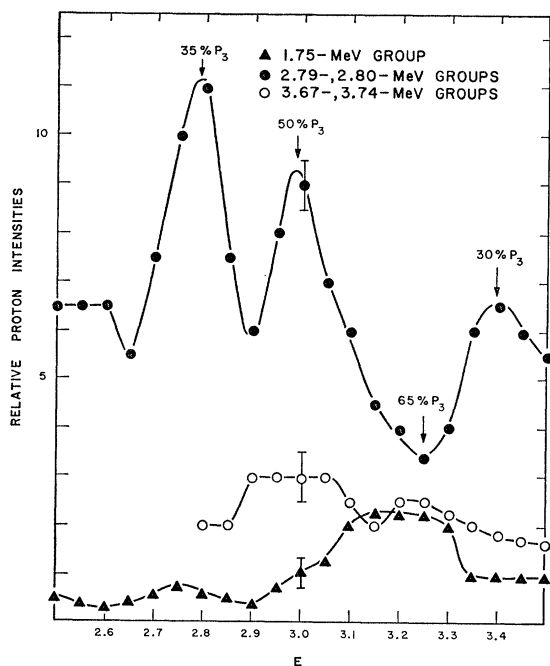


FIG. 4. Relative intensities of  $\text{Ne}^{21}$  proton groups observed at  $\theta_p = (165 \pm 6)^\circ$  as a function of the deuteron bombardment energy when employing a 0.04-mil-thick nickel entrance window. The relative intensities of the unresolved 2.790- and 2.797-MeV proton groups viewed in this geometry at several energies were determined from coincidence studies and are indicated as the percentage of the 2.790-MeV group ( $p_3$ ).

Isolated coincidence spectra were also obtained at  $E_d = 2.80, 3.25,$  and  $3.40$  MeV, these measurements being carried out to determine the relative populations of the 2.790- and 2.797-MeV states in this (colinear) geometry.

Two-parameter  $p$ - $\gamma$  time-coincidence measurements were carried out in the manner discussed in Sec. III A. In the present study, the  $5 \times 5$ -in. NaI(Tl) crystal was positioned with its front face 16 cm from the target center and was placed at angles with respect to the beam (and proton detector) axis of  $\theta_\gamma = 0^\circ, 30^\circ, 45^\circ, 60^\circ,$  and  $90^\circ$ ;  $\theta_p = 0^\circ, 45^\circ,$  and  $90^\circ$  measurements were repeated once. Beam currents of 3 nA were used, and real-to-random ratios typified by 20:1 were observed for  $p$ - $\gamma$  coincidences. The elapsed time for each correlation point measurement was 2 h.

Spectral reduction procedures were as outlined in Sec. III A. In most cases, the angular correlations were extracted from the data in straightforward fashion, normalization of the various data points being made according to the total beam charge deposited in the Faraday cup at the rear of the chamber. However, in order to obtain the angular correlation involving the  $2.790 \rightarrow 0$  distribution, it was necessary to remove the  $2.797 \rightarrow 0$  distribution from the observed, unresolved composite. By comparison of the relative intensities of the 2.45- and 2.80-MeV  $\gamma$  rays observed in the spectra integrated over angle with the branching-ratio informa-

tion on the 2.790- and 2.797-MeV states (Table II), it was found that only  $\sim 20\%$  of the 2.80-MeV photopeak was associated with the  $2.790 \rightarrow 0$  transition, the remaining  $\sim 80\%$  being associated with the  $2.797 \rightarrow 0$  radiation. Since this latter transition originates from a  $J = \frac{1}{2}$  state (Sec. II), its distribution is isotropic. Consequently, the  $2.790 \rightarrow 0$  distribution was obtained by isotropic subtraction of this  $2.797 \rightarrow 0$  contribution from the observed 2.80 MeV  $\gamma$ -ray photopeak. The method of least squares was applied to fit all of the observed correlations with the following even-order Legendre polynomial expansion:

$$W(\theta) = a_0 + a_2 P_2(\cos\theta) + a_4 P_4(\cos\theta). \quad (1)$$

The goodness of fit so obtained to each correlation is expressed in the usual  $\chi^2$  presentation.<sup>18</sup> Table III summarizes the fits of Eq. (1) to the correlation data.

The observed correlations were then fitted with the appropriate theoretical correlation expressions in a manner similar to that described by Poletti and Warburton.<sup>18</sup> Method II geometry<sup>17</sup> restricts populated  $\text{Ne}^{21}$  substates relative to the beam axis to be either  $\alpha = \frac{1}{2}$  or  $\frac{3}{2}$  in magnitude in the present reaction, and the absence of polarization sensitivity in the present experiment restricts the populations further in that  $P(-\alpha) = P(+\alpha)$ . Deviations of the experimental geometry from colinearity were considered in the fitting procedure by allowing  $P(|\frac{5}{2}|)$  to be  $\leq 10\%$  of  $P(|\frac{1}{2}|) + P(|\frac{3}{2}|)$ .<sup>17,18</sup> Employing these population parameters as variables best fits were obtained to the individual experimental correlations by the linear method of least squares for selected spin sequences and discrete values of the multipole amplitude ratio  $x$ . For each spin sequence considered, best fits were first obtained for values of  $\arctan x$  between the limits  $-90^\circ$  and  $90^\circ$  in  $5^\circ$  steps; in order to establish accurately positions of minima in  $\chi^2$  versus  $\arctan x$ , certain regions were stepped over in  $1^\circ$  steps. Where appropriate, similar analyses were carried out in simultaneously fitting two or three dependent correlation sets. In such cases, all except one

TABLE III. Results of even-order Legendre polynomial least-squares fits to  $\gamma$ -ray angular distributions in  $\text{Ne}^{21}$ .

$E_i$ (MeV)	Transition	$a_2/a_0$	$a_4/a_0$	$\chi^2$
0.350	$0.350 \rightarrow 0$	$-(0.36 \pm 0.02)$	$+(0.05 \pm 0.05)$	0.9
1.75	$1.75 \rightarrow 0.350$	$-(0.44 \pm 0.03)$	$+(0.02 \pm 0.03)$	0.2
1.75	$0.350 \rightarrow 0$	$-(0.28 \pm 0.05)$	$+(0.04 \pm 0.05)$	0.3
2.79	$2.79 \rightarrow 0$	$-(0.01 \pm 0.09)$	$-(0.04 \pm 0.10)$	2.0
2.79	$2.79 \rightarrow 0.350$	$+(0.02 \pm 0.04)$	$-(0.01 \pm 0.04)$	1.0
2.79	$0.350 \rightarrow 0$	$-(0.02 \pm 0.03)$	$-(0.04 \pm 0.03)$	0.2
2.80	$2.80 \rightarrow 0$	assumed isotropic		
3.67	$3.67 \rightarrow 0.350$	$-(0.21 \pm 0.03)$	$-(0.01 \pm 0.03)$	0.9
3.67	$3.67 \rightarrow 2.79$	$-(0.16 \pm 0.05)$	$-(0.02 \pm 0.06)$	0.2
3.67	$2.79 \rightarrow 0.350$	$-(0.01 \pm 0.06)$	$-(0.02 \pm 0.07)$	0.1
3.74	$3.74 \rightarrow 0$	$-(0.39 \pm 0.02)$	$-(0.05 \pm 0.03)$	1.5
3.89	$3.89 \rightarrow 0.350$	$+(0.12 \pm 0.04)$	$-(0.03 \pm 0.05)$	0.1
3.89	$0.350 \rightarrow 0$	$-(0.22 \pm 0.03)$	$+(0.01 \pm 0.03)$	3.2

<sup>18</sup> A. R. Poletti and E. K. Warburton, Phys. Rev. **137**, B595 (1965).

of the involved multipole amplitude ratios were specified from previous single-correlation results, and the goodness of fit obtained in these "two- and three-distribution fits" was obtained as a function of the remaining (unfixed) multipole amplitude ratio. Related spin and multipole amplitude ratio determinations resulting from the present studies are presented in the ensuing subsections and are summarized in Table IV.

### 1. The 0.350-MeV State

A  $J^\pi = \frac{5}{2}^+$  assignment has been firmly established for this state by previous studies,<sup>2,10,11</sup> and the transition to the  $\frac{3}{2}^+$  ground state is known to be predominantly dipole in character.<sup>1,6,12</sup> Accepting the above spin assignments, analysis of the correlation involving the  $0.350 \rightarrow 0$  transition indicates a solution consistent with these previous results, although the restriction on  $x$  from the present studies is not comparably stringent (see Table IV).

### 2. The 1.75-MeV State

$J = \frac{7}{2}$  has been previously established in three independent determinations for this state,<sup>1,2,6</sup> and the multipole amplitude ratio for the predominant  $1.75 \rightarrow 0.350$  cascade transition as obtained by averaging the values from these three studies is  $x = +(0.12 \pm 0.02)$ . Considering  $J = \frac{1}{2}$  through  $\frac{11}{2}$  assignments for the 1.75-MeV state and selecting  $x = +(0.02 \pm 0.02)$  for the  $\frac{5}{2}^+$ ,  $0.350 \rightarrow \frac{3}{2}^+$ ,  $0$  transition, a value indicated by several previous determinations,<sup>1,2,6</sup> the simultaneous two-distribution fit involving the  $1.75 \rightarrow 0.353 \rightarrow 0$  cascade transitions indicates an unambiguous  $J = \frac{7}{2}$  assignment for the 1.75-MeV state and also  $x = +(0.11 \pm 0.03)$  for the  $1.75 \rightarrow 0.350$  transition. These results are in excellent agreement with the previous ones.

### 3. The 2.790-MeV State

Pronko *et al.*<sup>9</sup> have recently assigned  $J = \frac{3}{2}$  to this level on the basis of angular correlation measurements in the  $\text{O}^{18}(\alpha, n\gamma)\text{Ne}^{21}$  reaction. As indicated in Table III, in the present study all radiations observed following formation of this state, whether populated directly or by  $\gamma$ -ray cascade, appeared isotropic within experi-

TABLE IV. Multipole amplitude ratios for  $\text{Ne}^{21}$   $\gamma$ -ray transitions as observed in the present studies.

$E_i$ (MeV)	$E_f$ (MeV)	$J_i$	$J_f$	Multipole amplitude ratio <sup>a</sup>
0.350	0	$\frac{5}{2}$	$\frac{3}{2}$	$-0.08 \leq x \leq +0.50, +2.5 \leq x \leq +3.3$
1.75	0.350	$\frac{7}{2}$	$\frac{5}{2}$	$+0.08 \leq x \leq +0.14$
3.67	0.350	$\frac{3}{2}$	$\frac{5}{2}$	... <sup>b</sup>
3.67	0.350	$\frac{5}{2}$	$\frac{5}{2}$	$+0.58 \leq x \leq +1.1, x \geq +3.0$
3.67	2.79	$\frac{3}{2}$	$\frac{5}{2}$	... <sup>b</sup>
3.67	2.79	$\frac{5}{2}$	$\frac{3}{2}$	$-0.10 \leq x \leq 0, x \geq +3.2$
3.74	0	$\frac{5}{2}$	$\frac{3}{2}$	$0 \leq x \leq +0.62, +1.7 \leq x \leq +2.5$

<sup>a</sup> Limits imposed to one standard deviation.

<sup>b</sup> Essentially no restriction imposed by the present studies.

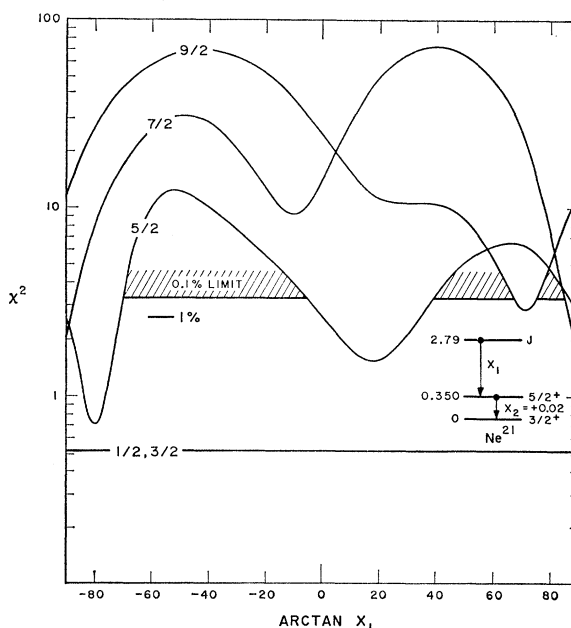


FIG. 5. Two-distribution fit concerning the 2.790-MeV state.  $\chi^2$  as a function of  $\arctan x_1$ , where  $x_1$  is the mixing ratio for the  $2.790 \rightarrow 0.350$  transitions, is illustrated for simultaneous fits to the  $2.790 \rightarrow 0.350$  and  $0.350 \rightarrow 0$  distributions under the assumptions presented in the inset energy-level diagram and discussed in the text. The shaded region represents the 0.1% statistical confidence limit, and the 1% limit is also indicated.

mental uncertainties. Considering  $J = \frac{1}{2}$  through  $\frac{9}{2}$  assignments for the 2.790-MeV state and again selecting  $x = +(0.02 \pm 0.02)$  for the  $\frac{5}{2}^+$ ,  $0.350 \rightarrow \frac{3}{2}^+$ ,  $0$  transition, the simultaneous two-distribution fit involving the  $2.790 \rightarrow 0.350 \rightarrow 0$  cascade transitions is illustrated in Fig. 5 and indicates acceptable solutions for  $J \leq \frac{7}{2}$ . Choosing  $J = \frac{1}{2}$  through  $\frac{7}{2}$  for the 2.790-MeV state and mixing ratio values for the  $2.790 \rightarrow 0.350$  transition consistent with the above two-distribution results, the  $2.790 \rightarrow 0.350 \rightarrow 0$  cascade transitions and the  $2.790 \rightarrow 0$  transition were simultaneously fit, the mixing ratio in the latter transition being variable. The results exclude  $J = \frac{7}{2}$  with  $>99.9\%$  statistical confidence, and so  $J \leq \frac{5}{2}$  for the 2.790-MeV state results from the present study.

### 4. The 3.67-MeV State

As explained in Sec. I, the present limitation on the spin of the 3.67-MeV level is  $J \geq \frac{3}{2}$ . The first step in analyses concerning this state was to fit the correlation involving the  $3.67 \rightarrow 0.350$  transition for assumed assignments  $J = \frac{1}{2}$  through  $\frac{11}{2}$  for the 3.67-MeV state. The results allowed  $J = \frac{3}{2}, \frac{5}{2},$  or  $\frac{7}{2}$  for this state, the other considered  $J$  values being excluded with  $>99.9\%$  statistical confidence. The next step was to obtain simultaneous fits to the observed correlations involving the  $3.67 \rightarrow 0.350$  and  $3.67 \rightarrow 2.790$  transitions under the following conditions: (1) It was accepted that  $J = \frac{3}{2}, \frac{5}{2},$  or  $\frac{7}{2}$  for the 3.67-MeV state and  $J = \frac{3}{2}$  for the 2.790-



MeV state<sup>9</sup>; (2) the relative population parameters for the 3.67-MeV state consistent with the acceptable solutions for the above-discussed 3.67  $\rightarrow$  0.350 correlation were effectively specified by stating discrete values of the associated multipole amplitude ratio with each of the three  $J$  values considered. In the case  $J = \frac{7}{2}$ , acceptable solutions were obtained only with  $x > 0.5$  for the 3.67  $\rightarrow$  2.790 transition. The crude lifetime limitation of 60 nsec imposed by the resolving time of the fast coincidence circuit is sufficient to exclude rigorously octupole admixtures of such magnitude for the transition in question, and so  $J = \frac{7}{2}$  is eliminated for the 3.67-MeV state by this analysis. Acceptable solutions were obtained for both  $\frac{3}{2}$  and  $\frac{5}{2}$  assignments to this level; associated limitations on the multipole amplitude ratio so obtained are given in Table IV. The final step in the analyses was to obtain simultaneous three-distribution fits to the correlations involving the 3.67  $\rightarrow$  2.790  $\rightarrow$  0.350  $\rightarrow$  0 cascade transitions. The value  $x = +(10 \pm 5)$  for the 2.790  $\rightarrow$  0.350 transition as reported by Pronko *et al.*<sup>9</sup> was assumed, and the multipole amplitude ratio for the 3.67  $\rightarrow$  2.790 transition was

again treated as the variable one. The results of this fit did not place further restriction on either the spin or the associated values of the multipole amplitude ratio, and so the present study indicates  $J = \frac{3}{2}$  or  $\frac{5}{2}$  as possible spins for the 3.67-MeV state.

### 5. The 3.74-MeV State

The 3.74-MeV  $\text{Ne}^{21}$  state has previously<sup>2</sup> been identified as the mirror level of the 3.54-MeV  $\text{Na}^{21}$  state, for which a  $J = \frac{5}{2}$  assignment has been shown most probable.<sup>19</sup> The angular correlation involving the predominant (94% relative intensity  $\gamma$ -ray branch) 3.74  $\rightarrow$  0 transition was fitted for  $J = \frac{1}{2}$  through  $\frac{9}{2}$  assignments assumed for the 3.74-MeV level. The results, which are illustrated in Fig. 6, establish  $J = \frac{3}{2}$  or  $\frac{5}{2}$  for the state with  $> 99.9\%$  statistical confidence. Consequently, the  $J = \frac{5}{2}$  assignment to this state based on mirror pair arguments<sup>2</sup> is in accord with this correlation result.

### 6. The 3.89-MeV State

The angular correlations involving the 3.89  $\rightarrow$  0.350  $\rightarrow$  0 cascade transitions were retrieved from the data and subsequently analyzed in a two-distribution fit with  $J = \frac{1}{2}$  through  $\frac{9}{2}$  assignments considered for the 3.89-MeV state, which was weakly populated in the present study. Acceptable solutions were obtained for  $J = \frac{3}{2}, \frac{5}{2}, \frac{7}{2}$  assignments. Since the correlation involving the 3.89  $\rightarrow$  0 transition, which represents a weak (23%) branch, could not be reliably retrieved from the data because of poor statistics, no further information was obtained on this state.

### C. Summary

As is evident in Table II, the branching-ratio information on the 1.75-, 2.87-, 3.67-, 3.89-, and 4.73-MeV states obtained from the present study on the  $\text{Ne}^{20}(d, p\gamma)\text{Ne}^{21}$  reaction essentially agrees within statistical uncertainties with that obtained from previous studies on the  $\text{F}^{19}(\text{He}^3, p\gamma)\text{Ne}^{21}$  and/or  $\text{O}^{18}(\alpha, n\gamma)\text{Ne}^{21}$  reactions.<sup>1,3,9</sup> The discrepancy which appears between the branching ratio for the 3.74-MeV state as reported in the present study and in a previous  $\text{F}^{19}(\text{He}^3, p\gamma)\text{Ne}^{21}$  study<sup>3</sup> may be attributed to the fact that this state was populated weakly relative to the close-lying 3.67- and 3.89-MeV levels in the previous measurement; subsequent extraction of this branching ratio in that study was necessarily attended by relatively large estimated uncertainties.<sup>4</sup> In the present study, the 3.74-MeV state was populated strongly relative to the adjacent levels (see Fig. 3), and the branching ratio was obtained without difficulty. The branching ratio obtained for the 4.44-, 4.53-MeV level composite via a previous study<sup>3</sup> on the  $\text{F}^{19}(\text{He}^3, p\gamma)\text{Ne}^{21}$  reaction established that the principal  $\gamma$  de-excitation mode for the 4.44-MeV state is a 1.57-

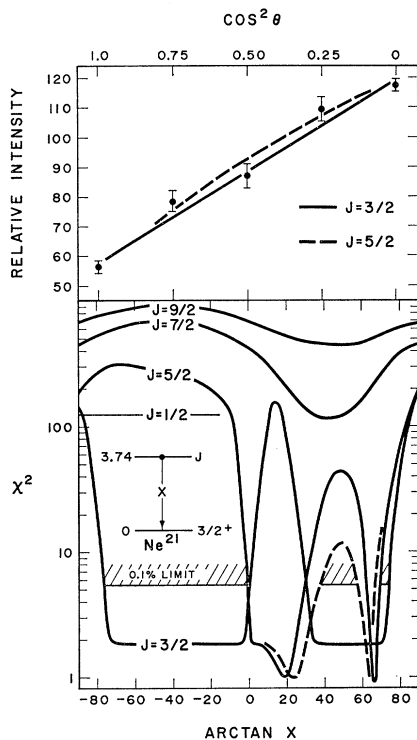
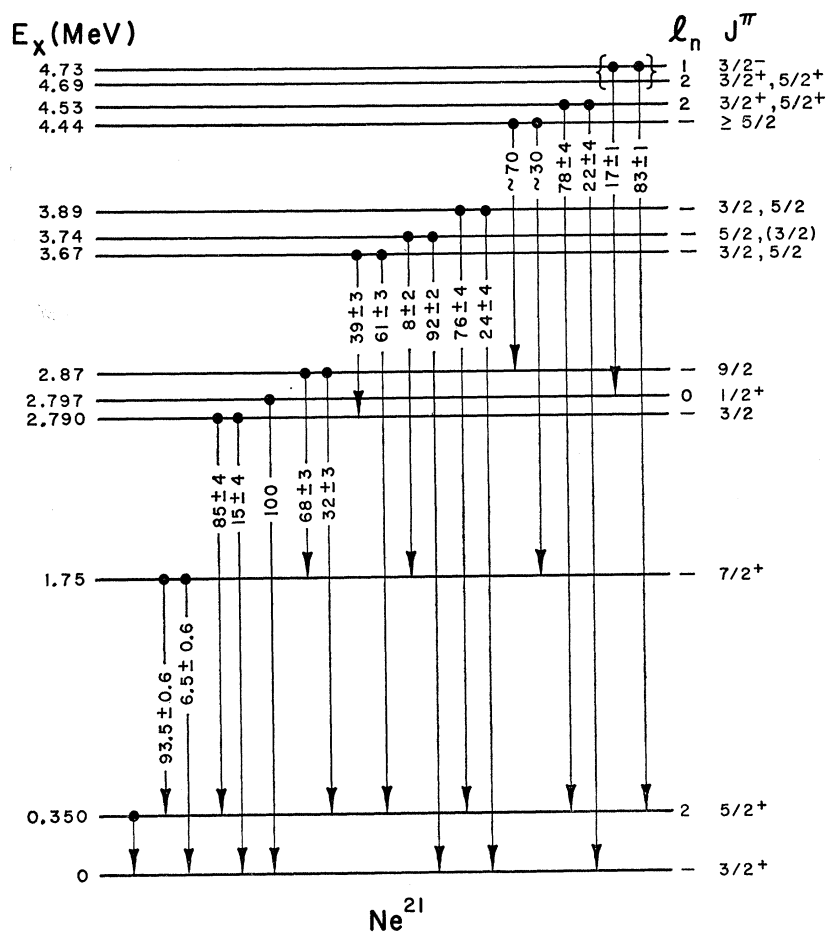


FIG. 6. Correlation results for the 3.74  $\rightarrow$  0 transition. The upper portion of the figure displays the data for the correlation obtained for the 3.74  $\rightarrow$  0 transition, and the lower portion illustrates  $\chi^2$  as a function of  $\arctan x$  for  $J = \frac{1}{2}$  through  $\frac{9}{2}$  assignments to the 3.74-MeV state. In the lower portion, the line below the shaded region represents the 0.1% statistical confidence limit, and the dashed curve represents the fit obtained by including the estimated maximum-finite-size effect in the fitting procedure. The curves in the upper portion correspond to the best fits (i.e., those fits associated with acceptable minima in  $\chi^2$ ) of the theoretical correlation functions to the observed correlation.

<sup>19</sup> C. Van der Leun and W. L. Mouton, *Physica* **30**, 333 (1964).

FIG. 7. Summary energy-level diagram for  $\text{Ne}^{21}$ . The branching ratios are the averages of the previous and present results as compiled in Table II. The  $l_n$  values are from Ref. 10, and the  $J^\pi$  limitations are the composite of those presented in Table I and those deduced in the present study.



MeV transition to the 2.87-MeV state. This result clearly negates the suggestion drawn from a previous  $\gamma$ - $\gamma$  coincidence study<sup>2</sup> on the  $\text{Ne}^{20}+d$  reaction that the principal decay mode for the 4.44-MeV level was a 1.64-MeV transition into the 2.790-, 2.797-MeV level composite. Furthermore, the 4.44-MeV level was not perceptibly populated in the present  $\text{Ne}^{20}(d,p\gamma)\text{Ne}^{21}$  branching-ratio studies. It is concluded that the origin of the 1.63-MeV photopeak previously observed in coincidence with  $\gamma$  radiations falling in the vicinity of 2.80 MeV in the  $\text{Ne}^{20}+d$   $\gamma$ -ray spectrum was misidentified<sup>2</sup>; while the origin of this 1.63-MeV  $\gamma$ -ray is presently unknown, it does not appear to emanate from a state below an excitation energy of 5 MeV in  $\text{Ne}^{21}$ . As described in footnote b of Table II, the branching ratios associated with each of the 4.44- and 4.53-MeV states were obtained by combining the previous  $\text{F}^{19}(\text{He}^3,p\gamma)\text{Ne}^{21}$  and present  $\text{Ne}^{20}(d,p\gamma)\text{Ne}^{21}$  results. The combined branching ratios for the 4.69- and 4.73-MeV states as determined in these two studies are in good agreement, and arguments presented elsewhere<sup>2</sup> strongly favor association of this branching ratio with the 4.73-MeV level. This preference is indicated by obvious notation in Fig. 7.

The studies presented in this section have provided further confirmation regarding the  $J^\pi = \frac{7}{2}^+$  assignment to the 1.75-MeV state as well as the  $x = + (0.12 \pm 0.02)$  mixing ratio for the  $1.75 \rightarrow 0.350$  transition, and only a  $J \leq \frac{5}{2}$  restriction is established for the 2.790-MeV level by the present studies. The  $J$  values for the 3.67-, 3.74-, and 3.89-MeV states have all been restricted to  $\frac{3}{2}, \frac{5}{2}$  by the present correlation results combined with previous ones.<sup>1,2</sup>

#### IV. DISCUSSION

Since the unpaired nucleon in an odd- $A$  nucleus plays a pronounced role as regards the Nilsson strong-coupling collective model representation of nuclear structure,<sup>20</sup> rotational band structures associated with nuclei having the same odd nucleon count  $\zeta$  are expected to be similar. A detailed intercomparison involving the experimentally observed and model-predicted properties associated with the lower-lying states in  $\text{Ne}^{21}$ ,  $\text{Na}^{21}$ , and  $\text{Na}^{23}$  lends strong support to this expectation in the  $\zeta = 11$  nuclear

<sup>20</sup> S. G. Nilsson, Kgl. Danske Videnskab. Selskab, Mat. Fys. Medd. 29, No. 16 (1955).

system,<sup>21</sup> and so an essential one-to-one correspondence between low-lying levels of the relatively well-studied Ne<sup>21</sup> and Na<sup>23</sup> nuclei is presently anticipated with some confidence. Thus apparent deviations from this correspondence between Ne<sup>21</sup> and Na<sup>23</sup> levels merit detailed scrutiny.

Considering experimental observations on Ne<sup>21</sup> first, the presently available information on the low-lying states of this nucleus is summarized in Tables I, II, and IV and in Fig. 7 of this paper. From the above-mentioned-model viewpoint, a crucial implication of the most recent studies on the low-lying levels of Ne<sup>21</sup> is the presence of only *one*  $J^\pi = \frac{1}{2}^+$  state among the 13 known levels below 5-MeV excitation energy: (1) The results of Pronko *et al.*<sup>9</sup> apparently eliminate  $J = \frac{1}{2}$  for the 2.790-, 2.87-, and 4.44-MeV states; (2) the present studies indicate  $J^\pi = \frac{1}{2}^+$  for the 2.797-MeV state and establish  $J > \frac{1}{2}$  for each of the three known states between 3- and 4-MeV excitation energy; and (3) the investigation of Pullen *et al.*<sup>10</sup> established  $J > \frac{1}{2}$  for each of the 4.53- and 4.69-MeV levels (see Table I and Fig. 7).

The known properties of the Na<sup>23</sup> states below 3-MeV excitation energy have been recently summarized and discussed by Poletti and Start.<sup>22</sup> Of prime interest in the present discussion, most probable assignments of  $\frac{1}{2}^+$  and  $\frac{1}{2}$  presently are associated with the Na<sup>23</sup> 2.39- and 2.64-MeV states, respectively. Poletti and Start<sup>22</sup> have emphasized that spins of  $\frac{3}{2}$  and of  $\frac{3}{2}$  and  $\frac{5}{2}$  have not been conclusively eliminated for these respective states, and a review of spectroscopic information available on each of these two states points out that the  $J = \frac{1}{2}$  assignment to the 2.64-MeV Na<sup>23</sup> state appears the more speculative of the two. An intercomparison of the energy-level diagram<sup>23</sup> for Ne<sup>21</sup> and Na<sup>23</sup> indicates that a definite and singular contrast now exists with respect to the "most probable" static properties of these two nuclei, namely the apparent difference regarding the location of  $J^\pi = \frac{1}{2}^{(+)}$  states in Ne<sup>21</sup> and Na<sup>23</sup>.

Considering Na<sup>23</sup> from the strong-coupling collective model viewpoint, calculations of the total nuclear binding energy<sup>21</sup> predict that the [12346]<sup>4</sup> [7]<sup>2</sup> 9-particle and the [1234]<sup>4</sup> [6]<sup>3</sup> [7]<sup>4</sup> hole configurations<sup>24</sup>

<sup>21</sup> A. J. Howard, J. P. Allen, and D. A. Bromley, Phys. Rev. **139**, B1135 (1965).

<sup>22</sup> A. R. Poletti and D. F. H. Start, Phys. Rev. **147**, 800 (1966).

<sup>23</sup> Compare, for example, Fig. 1 of Ref. 22 with Fig. 7 of the present work.

<sup>24</sup> The numbers here indicate the Nilsson orbits occupied by the 23 nucleons composing Na<sup>23</sup>. The corresponding Ne<sup>21</sup> configura-

should both generate  $K^\pi = \frac{1}{2}^+$  rotational bands, with the former unperturbed bandhead position lying  $\sim 1$  MeV below the latter one. This former configuration is also predicted to lie only  $\sim 3$  MeV below the [12346]<sup>4</sup> [7]<sup>2</sup> 11-particle configuration, which gives rise to a third  $K^\pi = \frac{1}{2}^+$  rotational band. Glöckle<sup>25</sup> considered the *two* lowest lying  $K^\pi = \frac{1}{2}^+$  configurations discussed above as well as the [12346]<sup>4</sup> [7]<sup>3</sup> and [12346]<sup>4</sup> [7]<sup>2</sup> 5-particle configurations, for which  $K^\pi = \frac{3}{2}^+$  and  $\frac{5}{2}^+$ , respectively, in a detailed model calculation concerning the static properties of the Na<sup>23</sup> states below 4-MeV excitation energy. A one-to-one correspondence between experimentally observed and model-predicted levels resulted, provided  $J^\pi = \frac{1}{2}^+$  assignments are accepted for *both* of the 2.39- and 2.64-MeV Na<sup>23</sup> states. Similar model calculations for Ne<sup>21</sup> and Na<sup>23</sup> carried out by Malik and Scholz<sup>26</sup> have taken into consideration all *three*  $K^\pi = \frac{1}{2}^+$  configurations cited above. The results are similar to that of Glöckle as concerns the two lowest-lying  $J^\pi = \frac{1}{2}^+$  states; they additionally indicate the presence of a third  $J^\pi = \frac{1}{2}^+$  state near 5-MeV excitation energy.

Thus a definite contrast presently exists not only between present experimental information on a particular static property of Ne<sup>21</sup> and Na<sup>23</sup> levels, but also between this information on the Ne<sup>21</sup> levels and the associated model predictions. Obvious confirmatory and further exploratory experiments are needed as the first step towards resolving these significant difficulties.

#### ACKNOWLEDGMENTS

We wish to thank C. K. Bockelman and J. R. Comfort for several illuminating discussions concerning the interpretation of the present particle distribution measurements and to J. R. Comfort for generating the PWBA computer fits to the associated data. We are grateful to D. J. Pullen, J. G. Pronko, and D. Pelte for valuable communications concerning their works prior to publication. We again wish to acknowledge the contribution of W. W. Watson concerning the mono-isotopic gas targets used for these studies. A. J. Howard, J. P. Allen, and D. A. Bromley express sincere appreciation to D. E. Alburger for his cordiality at the Brookhaven National Laboratory.

tions are [12346]<sup>4</sup> 9 and [1234]<sup>4</sup> [6]<sup>3</sup> [7]<sup>2</sup>, respectively. See Fig. 3 of Ref. 21 for quantitative results of the calculation.

<sup>25</sup> W. Glöckle, Z. Physik **178**, 53 (1964).

<sup>26</sup> F. B. Malik and W. Scholz, in Proceedings of the International Conference on Low-Energy Nuclear Physics, Dacca, 1966 (to be published); W. Scholz (private communication).